ASEAN Journal of Science and Engineering

Combined Pyrazole and Cu (II), Co (II) Metals: An Excellent Catalyst for Catecholase, Tyrosinase, Phenoxazinone Synthase, and Laccase for Oxygen Activation

Zakariae Abbaoui [1], Hasnae Arrass[1], Rachid Touzani[1,], Sana Ben Moussa[2], Abdullah Yahya Abdullah Alzahrani[2], Belkheir Hammouti[3]*

[1]University Mohammed Premier, Oujda, Morocco
[2]King Khalid University, Abha, Saudi Arabia.
[3]Euromed University of Fes, UEMF, Morocco
[*]Correspondence: E-mail: r.touzani@ump.ac.ma

ABSTRACT

This study explores the catalytic behavior of pyrazole-based copper (II) and cobalt (II) complexes as biomimetic models for key oxidative enzymes (Catecholase, tyrosinase, phenoxazinone synthase, and laccase for oxygen activation). The primary objective was to activate molecular oxygen and oxidize phenolic substrates through the use of structurally designed transition metal complexes. Complexes were prepared in situ and characterized using UV-Vis, FTIR, and XRD spectroscopy. The catalytic performance was evaluated in aerobic conditions and three solvents with differing polarities. Copper-based systems exhibited superior efficiency in mimicking enzymatic activities due to their favorable coordination properties. Because the acetate ligand allows easy substrate access to the metal center, Cu(II)-acetate complexes yielded the most effective oxidation outcomes. These findings suggest that rational design of metal-ligand systems inspired by natural enzymes can enhance selective oxidation reactions. The approach provides a science- and technology-driven foundation for environmentally benign catalysis in chemical and environmental applications

ARTICLE INFO

1. INTRODUCTION

Oxidation reactions are pivotal in organic synthesis, serving as essential steps to introduce desired functionalities into intermediates used in the production of high-value compounds such as pharmaceuticals, agrochemicals, and fine chemicals [1, 2]. For both economic and environmental reasons, molecular oxygen is the preferred oxidant in large-scale chemical industries [3, 4]. Its abundance in the air makes it a cost-effective and environmentally friendly option. However, large-scale oxidation processes often face challenges due to the use of heavy metals, associated thermal risks, and moderate chemo selectivity, especially when dealing with highly functionalized molecules [2, 5]. Traditional oxidation methods that rely on stoichiometric amounts of inorganic oxidants are not only toxic but also contribute significantly to environmental pollution. As a result, there has been increasing interest in catalytic systems capable of activating molecular oxygen efficiently while minimizing chemical waste. A key challenge in using molecular oxygen lies in its kinetic inertness. Organic substrates generally exist in a singlet ground state, while molecular oxygen in its triplet state is spin-forbidden for direct reactions.

However, if the organic substrate can be converted into a radical, the reaction becomes spin-allowed, facilitating oxygen activation. This can also be achieved through electron transfer from transition metal ions or potent organic electron donors such as flavins and pterins, which can generate reactive oxygen species [6, 7]. These organic cofactors have been extensively reviewed elsewhere and are beyond the scope of this discussion [8, 9]. One of the major challenges in using dioxygen for chemical transformations is its uncontrolled reactivity, which often results in low selectivity and over-oxidation. Nature has developed an elegant solution to overcome the kinetic barrier of dioxygen activation through the use of transition metals incorporated into proteins known as metalloenzymes [10, 11]. Among the various oxidative processes, the oxidation of alcohols to carbonyl compounds holds a prominent position in both laboratory research and industrial applications [12, 13]. Inorganic chemists have drawn inspiration from nature by designing catalysts that activate molecular oxygen, serving as small-molecule mimics of metalloenzymes to better understand their mechanistic pathways. Using principles of coordination chemistry, redox potentials, and electronic factors [10, 14, 15], enzyme donor sites are modelled with small organic molecules called ligands, which are then coordinated to metal centres to form complexes investigated as structural and functional analogues. Generally, many of these metal complexes exhibit promising catalytic activity [16]. However, a significant number of them may not be highly efficient in carrying out relevant oxidative organic transformations [2, 17]. Despite this, they remain valuable for providing critical insight into the mechanistic aspects of metalloenzymes. Over the past few decades, the development of catalytic systems aimed at mimicking enzymatic functions has been a central focus in bioinorganic chemistry. Beyond elucidating enzyme mechanisms, a long-term goal remains the design of metal complexes that can serve as efficient and practical catalysts.

Pyrazoles, which can be substituted with aromatic and heterocyclic groups, exhibit numerous biological activities that make them fascinating. Since the pioneering syntheses described by literature [18-21], the various pathways to accessing the pyrazole nucleus have undergone significant changes. In 1883, the term "pyrazole" to refer to a category of simple aromatic cycles in the heterocyclic series, distinguished by a five-membered ring structure consisting of three carbon atoms and two adjacent nitrogen atoms [18]. Pyrazoles are relatively rare alkaloids. Pyrazolyl-alanine, the first natural pyrazole isolated from pepper seeds, was discovered in 1959 (**Figure 1**) [22].
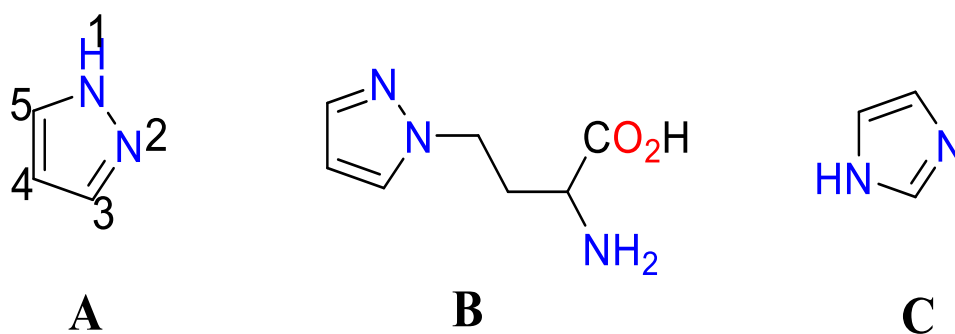
Figure 1. Pyrazole and 1-pyrazolyl-alanine

The term "pyrazole" was introduced by Ludwig Knorr in 1883. It is a five-membered aromatic heterocyclic ring consisting of three carbon atoms and two adjacent nitrogen atoms in positions 1 and 2 (**Figure 2**). It belongs to the alkaloid family. The proton of N (1)-H gives this atom an acidic character, while the nitrogen N (2) possesses a pair of electrons in an sp^2 orbital, giving it a basic character. In 1959, the first natural occurring pyrazole, 1-pyrazolyl-alanine, was isolated from watermelon seeds.
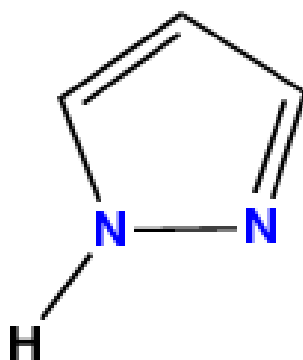

Figure 2. Structure of Pyrazole (L1)

2. METHODS
2.1. Materials

The organic compounds used in this study include catechol, 2-aminophenol, phenol, and 2,6-dimethylphenol. The metal salts used are as follows: Copper acetate $Cu(CH_3COO)_2$, Copper sulfate ($CuSO_4$), Copper nitrate (Cu $(NO_3)_2$), Cobalt nitrate (Co $(NO_3)_2$), and Copper chloride ($CuCl_2$), were used. The solvents employed in this study are Acetonitrile (CH_3CN), Methanol (MeOH), and Tetrahydrofuran (THF). These were obtained from commercial sources.

2.2. Methods

The prepared complex underwent various characterization methods. UV-Vis spectra were obtained using a UV-1900 I PC Shimadzu spectrometer. Additionally, X-ray diffraction (XRD) results were obtained using an XRD-6000 X-ray diffractometer, and Fourier-transform infrared (FTIR) spectroscopy was also performed.

2.3. Analysis and Characterization Techniques

Comprehensive characterization of the prepared complex was carried out. Fourier-transform infrared (FTIR) spectroscopy was performed in the 4500-400 cm^{-1} range using a Shimadzu infrared spectrophotometer, with samples prepared as pressed KBr pellets. For this purpose, 1 mg of the complex was finely ground with spectroscopic-grade (99% pure) KBr in a mortar. UV-Vis absorption spectra were recorded in the 200–800 nm range using a Shimadzu UV-1800 PC spectrophotometer, employing 1 cm path length glass cuvettes. X-ray diffraction (XRD) analysis was conducted using a Shimadzu XRD-6000 diffractometer to investigate the crystalline nature and phase purity of the complex.

2.4. Catalytic Activities

The experiments were conducted in methanol under ambient conditions using a UV-Vis UV-1900 I PC Shimadzu spectrometer at the Laboratory of Chemical Analysis and Environment. The absorbance of the substrates (catechol, aminophenol, phenol, 2,6-dimethylphenol) was monitored over a time range of 0 to 60 min at 390 nm for catechol and phenol, 430 nm for aminophenol, and 413 nm for 2,6-dimethylphenol. To prepare the complex formed in situ, a stepwise mixing approach was employed: 0.15 mL of a metal solution (2.10^{-3} mol/L) was mixed with 0.15 mL of a ligand solution (2.10^{-3} mol/L), or 0.3 mL of the prepared complex solution (2.10^{-3} mol/L) was used. Subsequently, 2 mL of substrate solution with a concentration of 10^{-1} mol/L, dissolved in 20 mL of MeOH, was added.

2.4. Kinetic Study

The kinetics of the oxidation reaction were studied to get more information on the catalytic efficiency of the complexes. This study was conducted to determine the kinetic parameters, such as V_{max} (maximum reaction rate) and K_m (reaction constant), using the initial rate method. The experiments were conducted in three different solvents (methanol (MeOH), tetrahydrofuran (THF), and acetonitrile (ACN)). In this approach, a solution of the in situ formed metal–ligand complex was treated with varying concentrations of each substrate (typically from 0.01 to 0.60 mol/L) under ambient conditions.

3. RESULTS AND DISCUSSION

Protein chemistry fascinates synthetic chemists, particularly due to the speed and remarkable selectivity of enzymatic reactions. This is especially true for the activation of molecular oxygen, a process catalyzed by specific metalloenzymes. This mechanism is crucial in biological systems, as it enables the use of atmospheric oxygen in controlled and selective oxidation reactions (**Figure 3**). The figure illustrates a catalytic oxidation process involving the activation of molecular oxygen (O₂) by a metal-based catalyst. This mechanism is inspired by the action of oxidative enzymes such as tyrosinase, laccase, phenoxazinone synthase, and catechol oxidase. In this system, various phenolic or aromatic substrates are oxidized by activated oxygen species, including: Phenol, 2,6-Dimethylphenol; 2-Aminophenol; and Catechol.

The catalytic properties of ligand complexes derived from pyrazole metals involving first-line metals such as Cu (II), Co (II) have recently been of great interest due to their extensive coordinating chemistry. Coordination chemistry. In our work, we have prepared several complexes using the complexation reaction of pyrazole with Cu (CH$_3$COO)$_2$, CuSO$_4$, and CuCl$_2$ metal salts. A mixture of 1 equivalent of Pyrazole with 1 equivalent of Cu (CH$_3$COO)$_2$, CuSO$_4$, and CuCl$_2$ in a few milliliters of methanol was stirred without heating, then the solvent was

evaporated for a few days. We obtained the following products (HA, HA_0, HA_1). After the evaporation of solvents in ambient conditions.
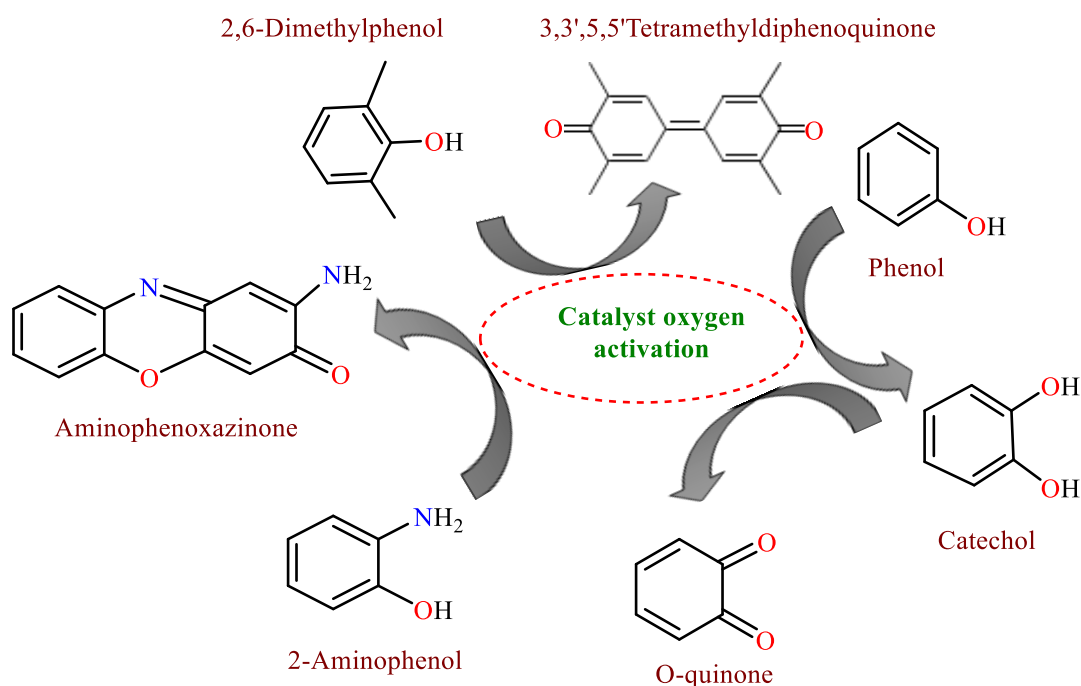

Figure 3. A representative scheme of the oxidative transformations discussed in this work.

The kinetic data from **Tables 1** and **2** allow comparison of the catalytic efficiency of pyrazole/based complexes associated with different copper salts ($CuSO_4$, $Cu(CH_3COO)_2$, and CuCl2 unspecified complex) in the oxidation of phenolic substrates in methanol. Analysis of the reaction rate (V), specific catalytic activity (a), and turnover (T) shows that the aminophenol substrate is the most reactive in all three cases. It exhibits the highest values of V, a, and T, indicating excellent affinity for the active centers of the studied complexes. The pyrazole/$CuSO_4$ complex stands out overall with the highest reaction rate (V = 38.02 µmol/L.min) and the largest turnover (T = 145,745 min^{-1}), especially for aminophenol. The pyrazole/$Cu (CH_3COO)_2$ complex shows better efficiency only for catechol, with V = 27.31 µmol/L.min, making it a particular case. The pyrazole/CuCl2 complex exhibits a maximum specific activity for aminophenol (V=32.47 µmol/L.min), demonstrating very high catalytic efficiency, and the largest turnover (T = 124500 min^{-1}), especially for aminophenol. Finally, the phenol and catechol substrates are generally less reactive than aminophenol and 2,6-dimethylphenol, with lower values of V and T in all systems studied.

Table 1. Kinetic data for the oxidation of substrates by complexes based on pyrazole and Metal salts in methanol [rate: V (µmol/L.min), Catalytic activity concentration b (µmol/L.min), activity: a (µmol/mg.min), and turnover: T (min^{-1}).

V (µmol/L.min)	b (µmol/mL.min)	a (µmol/min.mg)	T (min^{-1})

Catechol (HA_0)	16.39	125.70	251.69	62850
2,6-Dimethylphenol (HA0)	37.56	287.97	576.60	143985
Aminophenol (HA_0)	38.02	291.49	583.65	145745
Phenol (HA_0)	18.05	138.39	277.10	691995
Catechol (HA)	27.31	209.39	524.39	104695
Aminophenol (HA)	9.79	75.06	187.97	37530
Phenol (HA)	3.26	24.99	62.58	12495
Catechol (HA_1)	3.23	24.83	72.81	12415
2,6-Dimethylphenol	18.75	143.75	421.57	71875
Aminophenol	32.47	249	730.24	124500
phenol (HA_1)	15.92	122.10	358.08	61050

FTIR analysis is shown in **Table 3**. The IR spectrum of the pyrazole/CuSO₄ complex shows key absorption bands confirming complexation. Detailed information regarding IR is explained elsewhere [23-25]. A broad O–H band around 3400 cm⁻¹ indicates water molecules, likely coordinated to Cu²⁺. Peaks near 3100 cm⁻¹ correspond to aromatic C–H stretches from the pyrazole ring. Bands around 1600 and 1500 cm⁻¹ are attributed to C=N and C=C stretching in the pyrazole, while the region around 1100 cm⁻¹ suggests C–N vibrations. Strong bands near 1050 cm⁻¹ confirm the presence of sulfate (SO_4^{2-}). The IR spectrum of the pyrazole/copper (II) acetate complex confirms coordination between pyrazole and Cu²⁺. The broad O–H band at ~3400 cm⁻¹ suggests hydration. Aromatic C–H stretching bands appear near 3100 cm⁻¹. Shifts in the C=N and C=C bands (~1600 cm⁻¹) suggest that nitrogen from the pyrazole ring is coordinating with copper. The appearance of distinct COO⁻ asymmetric and symmetric stretches between 1550–1400 cm⁻¹ confirms the presence of acetate ligands. The IR spectrum of the pyrazole/CuCl₂ complex displays a broad band around 3200–3400 cm⁻¹, attributed to the N–H stretching vibration of the pyrazole ring. A slight shift of the C=N stretching band near 1600 cm⁻¹ suggests coordination of the pyrazole nitrogen to the copper (II) center.

XRD analysis is shown in **Table 4**. The numerous peaks in the 10–40° at 2θ region indicate a crystalline structure rich in distinct lattice planes. Hydrated copper sulfate (CuSO₄) typically crystallizes with intense peaks between 15 and 30°. The complexity of the profile and the multiple peaks suggest a likely polyphasic or highly complex structure, potentially resulting from coordination with the pyrazole ligand. The presence of intense peaks at low angles (around 7–12° at 2θ) suggests a large d-spacing, which is typically associated with layered structures or the inclusion of bulky organic ligands. In this case, coordination between Cu(CH₃COO)₂ and pyrazole likely leads to the formation of a supramolecular or polymeric structure with significant interplanar distances. This is consistent with the incorporation of pyrazole rings, which can induce steric hindrance and extend the unit cell dimensions. The resulting crystalline structure may be complex, possibly featuring hydrogen bonding or π–π interactions between pyrazole units, contributing to the observed diffraction pattern. The presence of particularly intense peaks between 8 and 12° at 2θ indicates a likely organometallic complex with an open or layered structure, characterized by large interplanar distances. This is typical for chlorinated transition metal complexes coordinated with azole-type ligands such as pyrazole. The sharp and well-defined diffraction peaks suggest high crystallinity and a structurally homogeneous phase, possibly reflecting a well-ordered coordination network formed between CuCl₂ and the pyrazole ligands. Such structures may involve bridging pyrazole units and extended supramolecular architectures, contributing to the observed diffraction pattern at low angles. Based on **Tables 2** and **3**, the schematic result is illustrated in **Figure 4**.

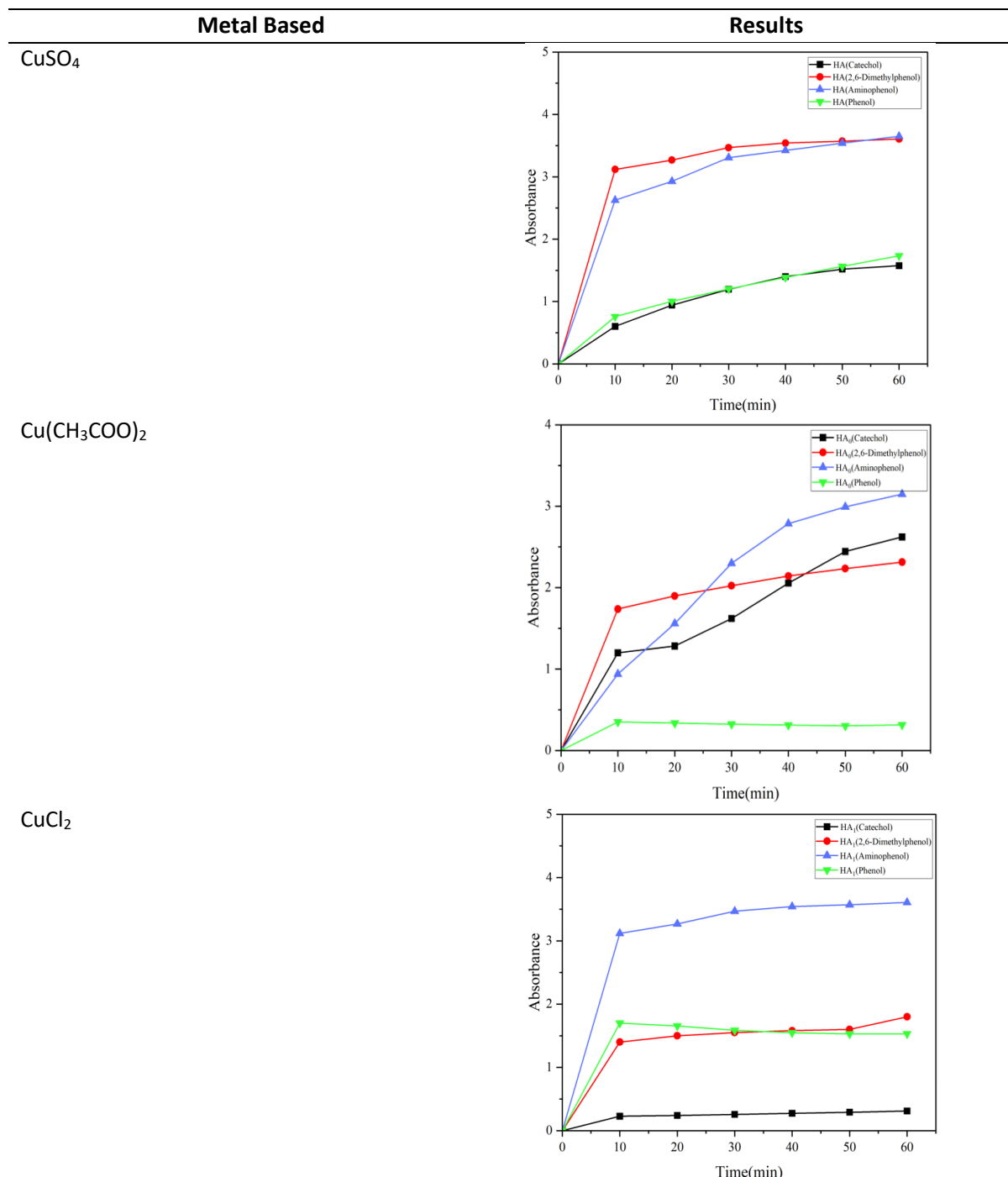**Table 2.** UV-Vis spectra of the ligand and its complexes based by metal.

Metal Based	Results
CuSO$_4$	
Cu(CH$_3$COO)$_2$	
CuCl$_2$	

Table 3. FTIR analysis

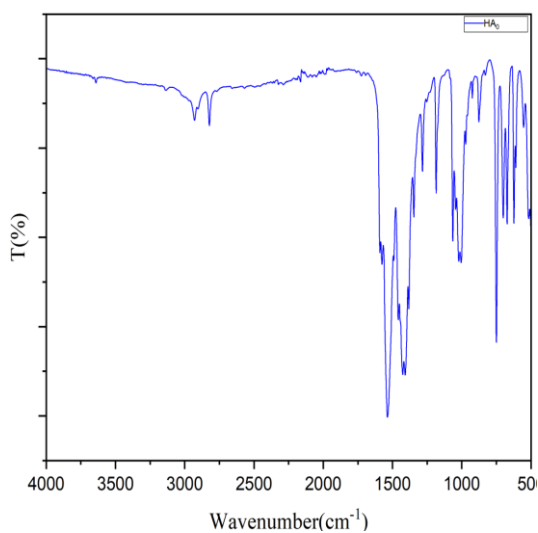| Sample ligand and its complexes	FTIR results

CuSO₄
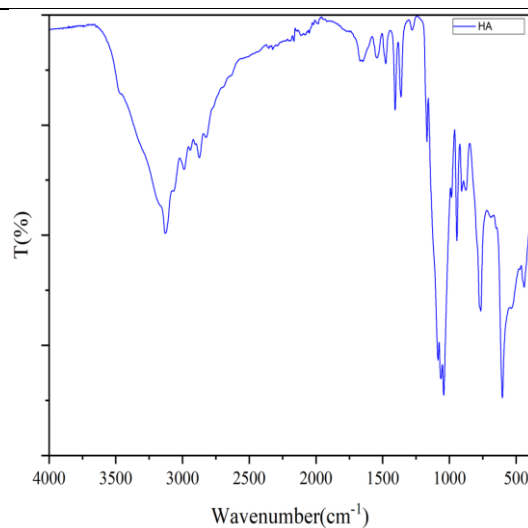
Cu(CH₃COO)₂
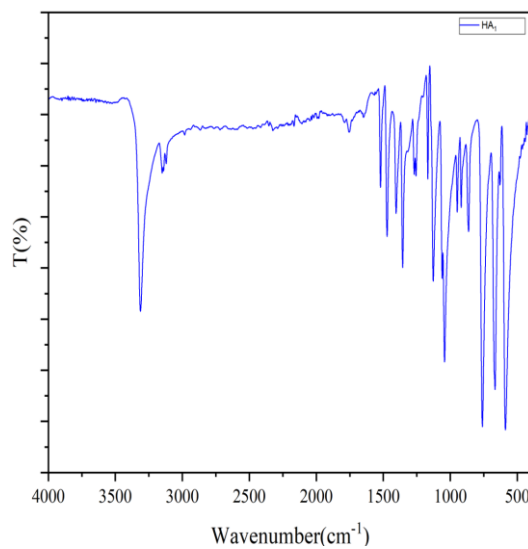
CuCl₂

Table 4. XRD analysis

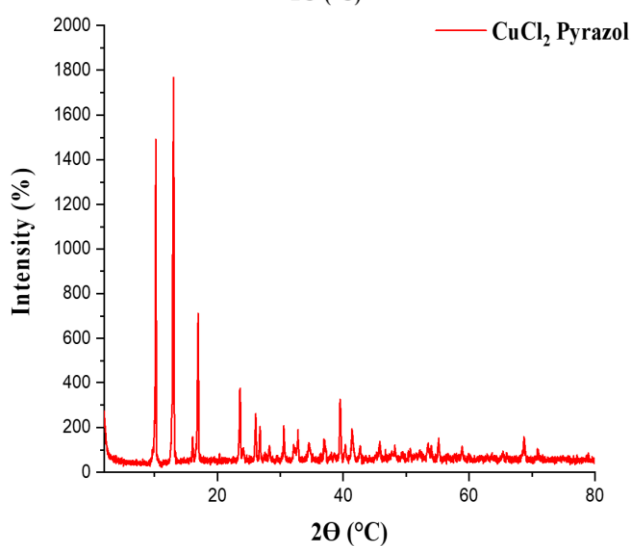| Sample ligand and its complexes	XRD analysis result

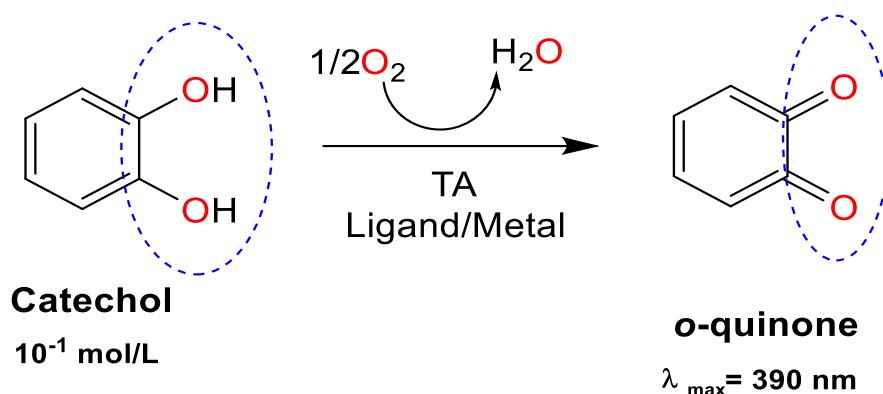CuSO$_4$
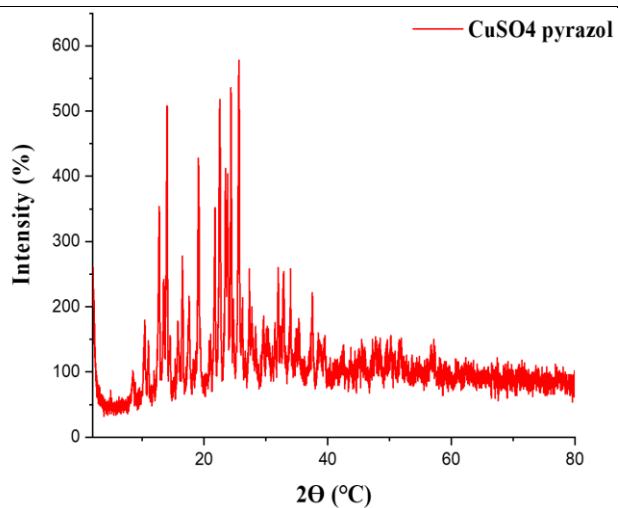
Cu(CH$_3$COO)$_2$
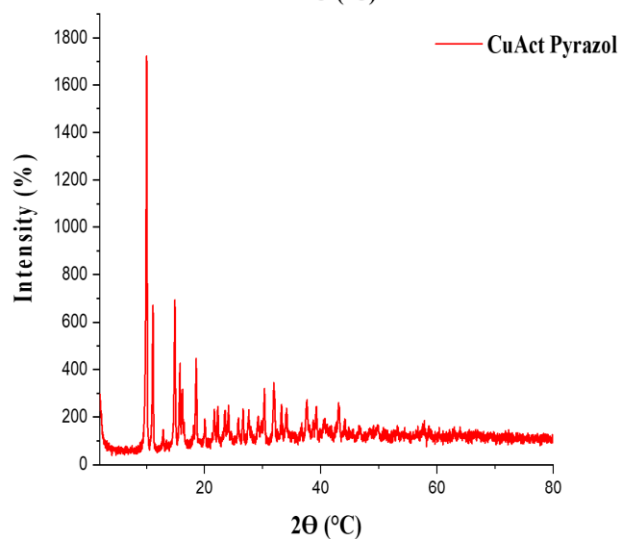
CuCl$_2$

Figure 4. Formation of o-quinone from catechol.

This study aims to develop a new and efficient pyrazole-based catalytic system through in situ complexation with selected transition metal salts, including CuCl₂, Cu (NO₃)₂, Co(NO₃)₂, Cu(CH₃COO)₂, and CuSO₄ which can be seen in **Figure 5(a-f)**. These complexes are evaluated for their catecholase like activity, specifically in the oxidation of catechol under ambient conditions. To assess the impact of solvent polarity on catalytic performance, three solvents with distinct physicochemical properties were employed: tetrahydrofuran (THF) as an aprotic apolar solvent, acetonitrile (CH₃CN) as an aprotic polar solvent, and methanol (CH₃OH) as a protic polar solvent. The overarching objective is to identify optimal catalyst-solvent systems capable of mimicking metalloenzyme function, thereby contributing to the development of sustainable and selective oxidation processes. Initially, the absorbance of o-quinone remains practically zero over time in the absence of a catalyst, indicating that the oxidation of catechol does not occur without a catalyst. with catechol in MeOH solvent. The results unequivocally demonstrate that the tested pyrazole-based, in the absence of a metal ion, is inactive in catalyzing catechol oxidation. However, upon addition of the pyrazole–metal salt mixture to the catechol solution, a notable increase in absorbance corresponding to o-quinone was observed, with a characteristic peak appearing around 390 nm. This outcome confirms the in-situ formation of the catalytically active metal–ligand complex. No catecholase activity was observed for the tested complexes in acetonitrile, whereas the catalytic results in methanol have been previously reported. provides a schematic illustration of the absorbance evolution over time during the oxidation of catechol, catalysed by in situ generated complexes formed between the pyrazole-based ligand and five different metal salts in methanol. **Table 5** presents the catechol oxidation rates catalyzed by in situ formed complexes using pyrazole-based ligands and various metal salts. The results indicate that complexes formed with copper (II) acetate [Cu(CH₃COO)₂], where one equivalent of ligand is combined with three equivalents of metal, exhibit the highest catalytic efficiency, with an oxidation rate of 17.156 µmol/L.min. In contrast, complexes formed with cobalt (II) nitrate [Co(NO₃)₂], where one equivalent of pyrazole ligand is combined with two equivalents of metal, show a lower catalytic activity, with a rate of 0.333 µmol/L.min. These variations demonstrate the influence of both the metal ion and the ligand structure on catalytic performance. Among the tested metal salts, Cu(CH₃COO)₂ proves to be the most efficient in mimicking catecholase activity, confirming the strong catalytic potential of copper-based systems.

The complexes showed the best catalytic activity due to the ease of metal coordination. Copper-based complexes, in particular, were the most efficient in oxidizing catechol. This is likely because the bond between the copper cation and the CH₃COO⁻ anion is relatively weak, allowing the substrate to easily replace the anion and interact with the metal. This weaker bond makes copper more effective than other transition metals in catalyzing catechol

oxidation. To confirm the significant catalytic activity of our in situ prepared complexes, we conducted kinetic studies to track the formation of o-quinone in the presence of L1/Cu (CH₃COO)₂ (1/3) complexes. At room temperature, we recorded the absorbance at λ = 390 nm every 5 minutes, and the results are shown in **Figure 6**. Our findings reveal that the pyrazole-copper acetate complexes exhibit considerable catalytic activity in converting catechol to o-quinone. The appearance of a distinct peak at 390 nm indicates the formation of the desired product, highlighting the efficiency of the complexes in catalysis. The kinetic data, showing a steady increase in absorbance over time, further supports the catalytic role of our compounds. In particular, the absorbance values for the L1/Cu (CH₃COO)₂ complexes increased more rapidly compared to others, which may be due to the fact that the enzyme catecholase, which catalyses a similar reaction, contains two copper ions at its active site.
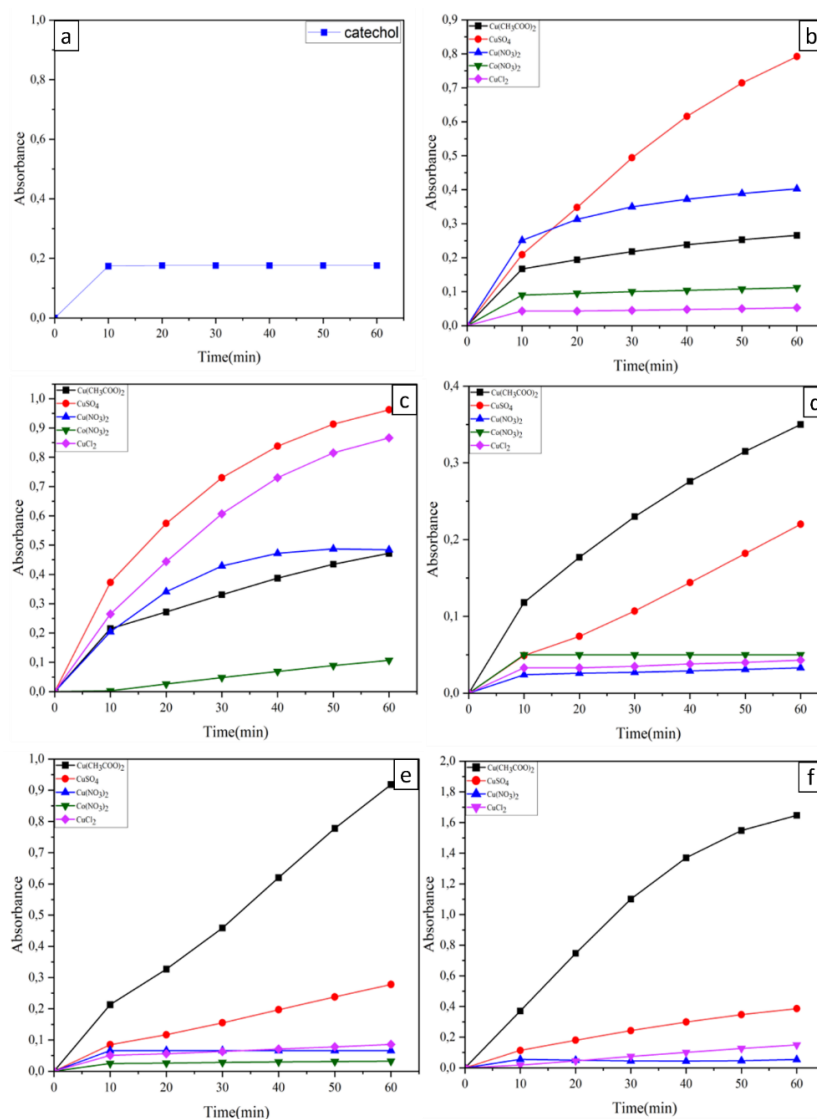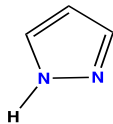

Figure 5. Oxidation of catechol (a) in the presence of complexes formed in situ by 1L/1M (b); 2L/1M (c); 3L/1M (d); 1L/2M (e); 1L/3M (f) in MeOH.

Table 5. Kinetic data for the oxidation of catechol by complexes based on pyrazole and different metal salts in methanol [rate: V (μmol. L^{-1}. min^{-1}), Catalytic activity concentration b (μmol. L^{-1}. min^{-1}), activity: a (μmol mg^{-1}.min^{-1}), and turnover: T (min^{-1})].

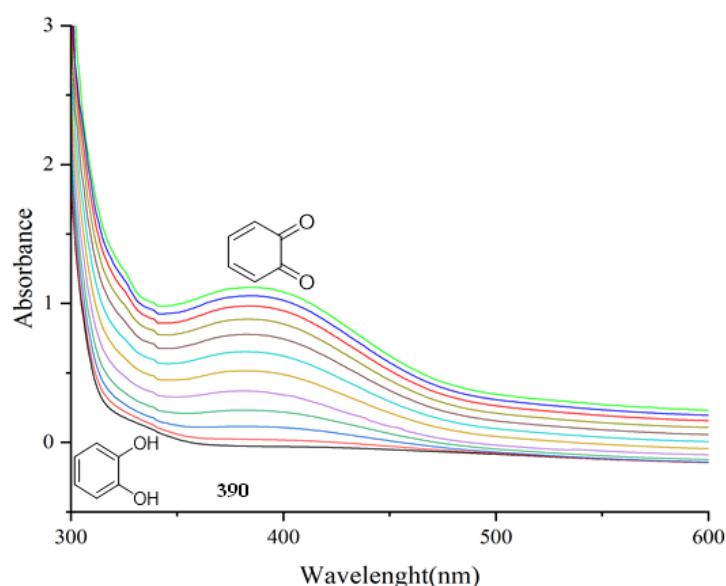| Ligands	Sels métalliques	V (μmol/L.min)	b (μmol/mL.min)	b (μmol/mL.min)	T (min^{-1})
	1L/1CuSO$_4$	8.25	63.25	126.64	31625
	2L/1CuSO$_4$	10.020	76.82	153.818	38410
	3L/1Cu (CH$_3$COO)$_2$	3.645	25.95	64.988	129795
	1L/2Cu (CH$_3$COO)$_2$	9.56	73.312	183.60	366656
	1L/3Cu (CH$_3$COO)$_2$	17.156	131.156	329.40	65756

Figure 6. Absorbance spectrum of o-quinone as a function of time for the 1L/3Cu (CH$_3$COO)$_2$ combination.

3.1. Catechol: Kinetic Study

A kinetic study was performed to determine the Michaelis-Menten constants, Km and Vmax, for the catechol oxidation reaction. This was done by plotting the initial reaction rate (Vi) as a function of the catechol substrate concentration. The study was conducted using a solution of the in situ prepared complex, with catechol concentrations ranging from 0.01 to 0.6 mol/L under ambient conditions. To determine Km and Vmax graphically, we used Michaelis-Menten plots, which allow for more accurate extrapolation of these constants. The reaction kinetics followed a typical Michaelis-Menten pattern. On the other hand, **Tables 6**, and **7**, clearly show that the K$_m$ values vary with the change of solvent. The combination of L1/CuCl2 proves to be the most efficient catalyst for the oxidation reaction under study. The K$_m$ values range from 0.002 mol/L in ACN, which appears to be the most suitable solvent for the catalytic study of this ligand series concerning catechol oxidation.

Table 6. Dependence of the reaction rates on the catechol (2 ml) concentrations varying 10-1 M to 6 × 10-1 M for the oxidation reaction catalysed by L/M complexes (0.3 ml; 2× 10-3 M) at 390nm.
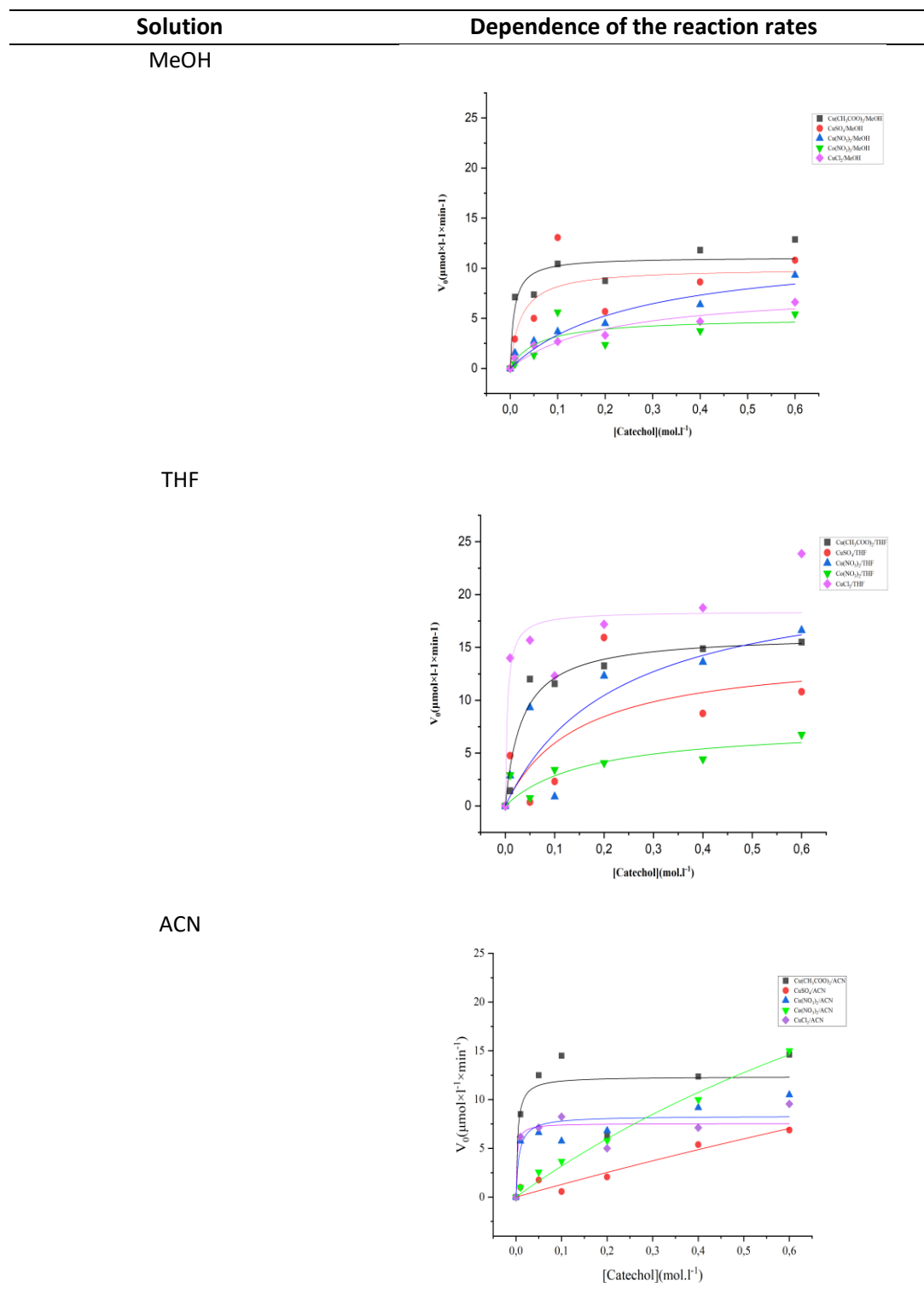
Solution	Dependence of the reaction rates
MeOH	
THF	
ACN	

Table 7. Kinetic parameters of the reaction.

ACN	Cu (CH$_3$COO)$_2$	CuSO4	Cu (NO$_3$)$_2$	Co (NO$_3$)$_2$	CuCl$_2$
V$_{max\ (MeOH)}$	12.62	10.65	9.24	4.59	5.94
K$_{m\ (MeOH)}$	0.018	0.029	0.027	0.04	0.12
V$_{max\ (THF)}$	15.54	12.86	17.42	6.05	18.27
K$_{m\ (THF)}$	0.03	0.10	0.14	0 .10	0.004
V$_{max\ (ACN)}$	12.21	7.05	8.21	14.61	7.50
K$_{m\ (ACN)}$	0.003	0.28	0.006	0.25	0.002

3.2. Catechol: Oxidation of Phenoxazinone in the Presence of a Complex in Situ

In nature, phenoxazinone synthase, a multicopper oxidase found naturally in the soil bacterium Streptomyces antibioticus, catalyzes the six-electron oxidative condensation of various derivatives of 2-aminophenol to produce the phenoxazinone chromophore (**Figure 7**).
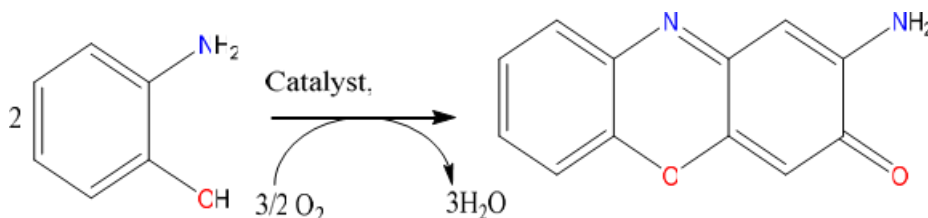
Figure 7. Formation of 2-aminophenoxazine-3-one (APX) from 2-aminophenol.

The objective of the analysis was to investigate complex formation by mixing 0.15 mL of a metal salt solution (2×10^{-3}mol·L^{-1}) with a ligand solution 2×10^{-3}mol·L^{-1}), followed by treatment with 2 mL of 2-aminophenol (0.10 mol/L) in an appropriate solvent under aerobic conditions, with Methanol (MeOH) chosen as the solvent. The kinetics of the reaction were monitored using a Shimadzu UV-1800 PC spectrophotometer at a constant temperature of 25 °C. Maximum absorbance was observed at 430 nm, with a molar extinction coefficient (ε) of 1600 L/mol cm in MeOH. This approach allowed for a detailed study of the kinetics of complex formation, utilizing MeOH as the solvent, followed by treatment with 2-aminophenol, with absorbance measurements recorded over time using the spectrophotometer (Meziane et al., 2024). These findings are also summarized in **Table 6.** In this study, we analysed the oxidation activity of 2-aminophenol using ligand pyrazole and various metal salts such as Cu(CH$_3$COO)$_2$, CuSO$_4$, Cu(NO$_3$)$_2$, Co(NO$_3$)$_2$, and CuCl$_2$, all dissolved in the solvent MeOH. The results show that catalytic activity varies significantly depending on the choice of ligand, salt and solvent. The L$_1$ complex and the metal salt L$_1$/CuSO4 (1/2), showed the highest catalytic activity in the MeOH solvent reaction rate, reaching 41.66 μmol·L^{-1}·min^{-1}, confirming its superior efficiency in promoting the oxidation process. These findings suggest that both the nature of the metal ion and its associated anion play a key role in mimicking phenoxazinone synthase-like activity.

To monitor the reaction kinetics, spectra were recorded every 10 minutes over the course of one hour, starting immediately after the addition of OAP to the solution containing the metal complexes. In the context of aminophenol oxidation, the results presented in **Figure 8 (a-f)** and **Table 8** highlight the strong influence of the metal salt on the catalytic activity of our chemical models. Among the tested systems, L1/CuSO$_4$ (1L/2M) exhibited the highest reaction rate, reaching 41.66 μmol·L^{-1}·min^{-1}, confirming its superior efficiency in promoting the oxidation process. These findings suggest that both the nature of the metal ion and its associated anion play a key role in mimicking phenoxazinone synthase-like activity. To verify the significant catalytic activity of our in situ prepared complexes, kinetic studies were

performed to monitor the formation of 2-aminophenoxazine-3-one in the presence of L1/CuSO$_4$ (1:2) complexes. Absorbance measurements were taken at λ = 430 nm at 5-minute intervals at room temperature, with the results presented in **Figure 9**. The data demonstrate that the pyrazole–copper sulfate complexes effectively catalyze the oxidation of aminophenol to 2-aminophenoxazine-3-one. The emergence of a distinct absorption peak at 430 nm confirms the formation of the target product and underscores the catalytic efficiency of the in situ generated complexes.
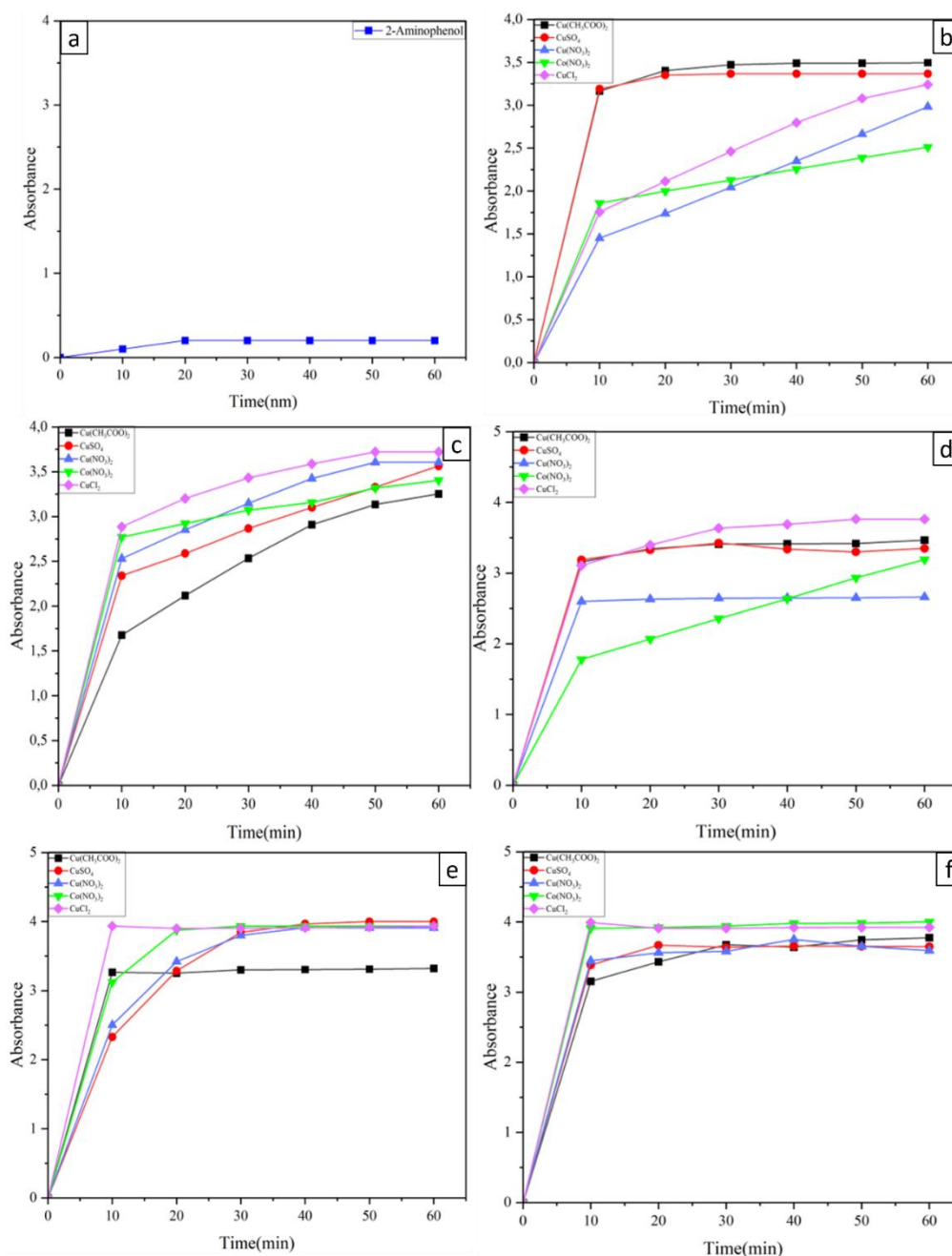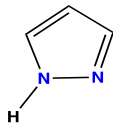

Figure 8. Oxidation of Aminophenol (a) in the presence of complexes formed in situ by 1L/1M (b); 2L/1M (c); 3L/1M (d); 1L/2M (e); 1L/3M (f) in MeOH.

Table 8. Kinetic data for the oxidation of Aminophenol by complexes based on pyrazole and different metal salts in methanol [rate: V (µmol/L.min), Catalytic activity concentration b (µmol/L.min), activity: a (µmol/mg.min), and turnover: T (min⁻¹)]

Ligands	Sels métalliques	V (µmol/L.min)	b (µmol/mL.min)	b (µmol/mL.min)	T (min⁻¹)
	1L/1Cu (CH₃COO)₂	35.78	274.32	687	137160
	2L/1CuCl₂	38.18	292.77	858.61	146385
	3L/1CuCl₂	39.19	300.51	881.31	150255
	1L/2CuSO₄	41.66	319.44	639.62	159720
	1L/3CO (NO₃)₂	41.65	319.36	548.58	159680
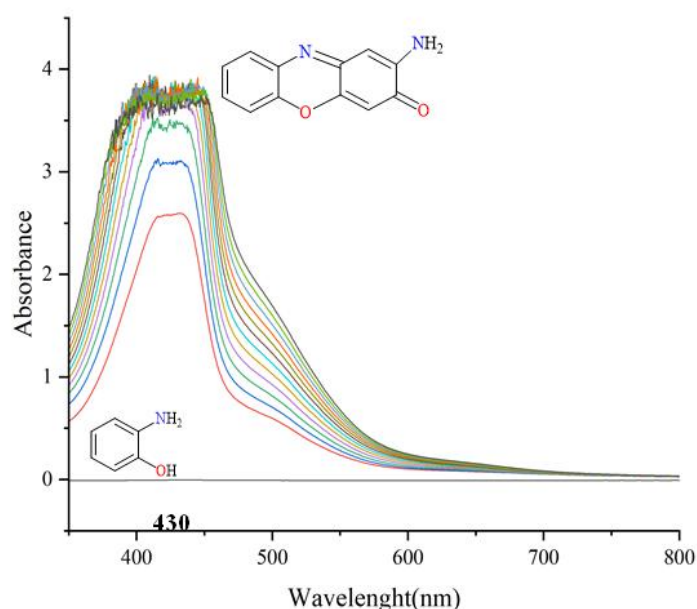
Figure 9. 2-aminophenoxazine-3-one absorbance recorded at a time interval of 10 min combination 1L/2CuSO₄.

3.3. Aminophenol: Kinetic Study

A kinetic study was carried out by determining the constants Km and Vmax of the oxidation reaction of aminophenol. The method consists of plotting the graph representing the Vi as a function of the substrate concentration (aminophenol). We carried out this study by using a solution of the combinations L1/Cu (CH₃COO)₂, L1/CuSO₄, L1/Cu (NO₃)₂, L1/Co (NO₃)₂ and L1/CuCl₂, treated with different concentrations 2-aminophenol (from 0.01 to 0.6 M) under ambient conditions. For the graphical determination of these two constants (K_m and V_{max}), there are Michaelis-Menten graphical representations, **Table 9** and **Table 10,** that present the results, allowing more precise extrapolations. By measuring the initial speed (V_0) of the reaction for different concentrations of the substrates, we constructed a graph of V_0 (µM/min) as a function of the variation in the concentration of the substrates (M), which allowed us to obtain the constants K_m and V_{max} for the different complexes formed in situ. The K_m values range from 0.0015 mol/L in THF of the combinations L_1/CuCl₂, which appears to be the most suitable solvent for the catalytic study of this ligand series with respect to Aminophenol oxidation.

Table 9. Dependence of the reaction rates on the aminophenol (2 ml) concentrations varying 10-1 M to 6 × 10-1 M for the oxidation reaction catalysed by L/M complexes (0.3 ml; 2× 10-3 M) at 430 nm in MeOH.
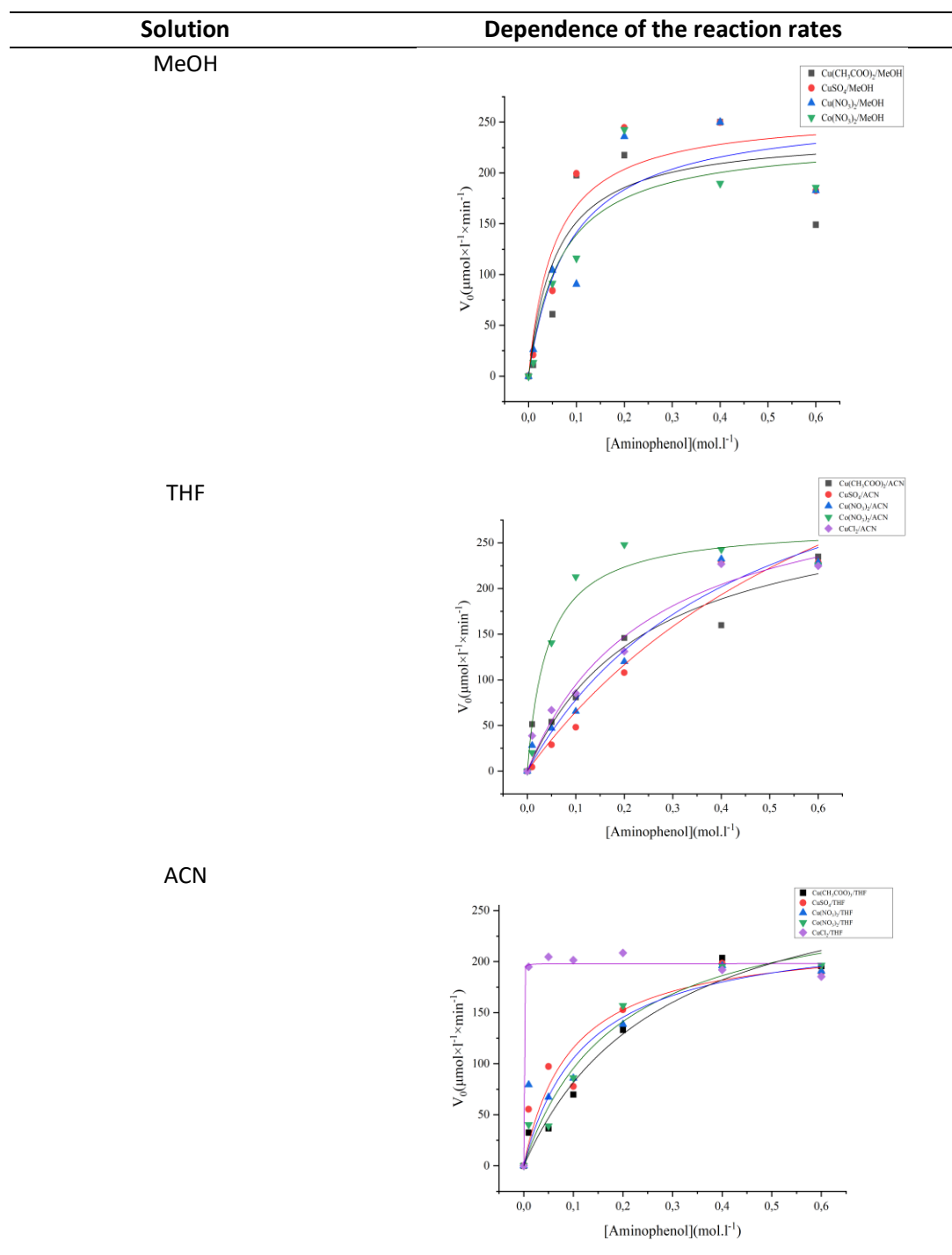
Solution	Dependence of the reaction rates
MeOH	
THF	
ACN	

Table 10. Kinetic parameters of the reaction.

ACN	Cu (CH₃COO)₂	CuSO4	Cu (NO₃)₂	Co (NO₃)₂	CuCl₂
$V_{max\ (MeOH)}$	218.70	237.04	229.65	210.63	235.69
$K_{m\ (MeOH)}$	0.048	0.044	0.065	0.054	0.056
$V_{max\ (THF)}$	210.89	194.18	195.38	208.18	198.09
$K_{m\ (THF)}$	0.14	0.07	0.08	0.11	0.0015
$V_{max\ (ACN)}$	215.93	247.51	245.06	252.74	237.17
$K_{m\ (ACN)}$	0.130	0.215	0.181	0.037	0.137

3.4. Aminophenol: Oxidation of Phenol in the presence of a complex in Situ

This study focused on evaluating the catalytic efficiency of various complexes formed between the pyrazole ligand and metals salts (Cu (CH₃COO)₂, CuSO₄, Cu (NO₃)₂, Co (NO₃)₂, CuCl₂) in the oxidation of phenol, a compound of major importance in fine chemistry and environmental treatment. The oxidation of phenol was carried out by successively adding 0.15 mL of the ligand (2.10^{-3} mol·L⁻¹) and 0.15 mL of the metal salt (2.10^{-3} mol·L⁻¹) to a solution containing phenol (10^{-1} mol·L⁻¹) (see **Figure 10**).
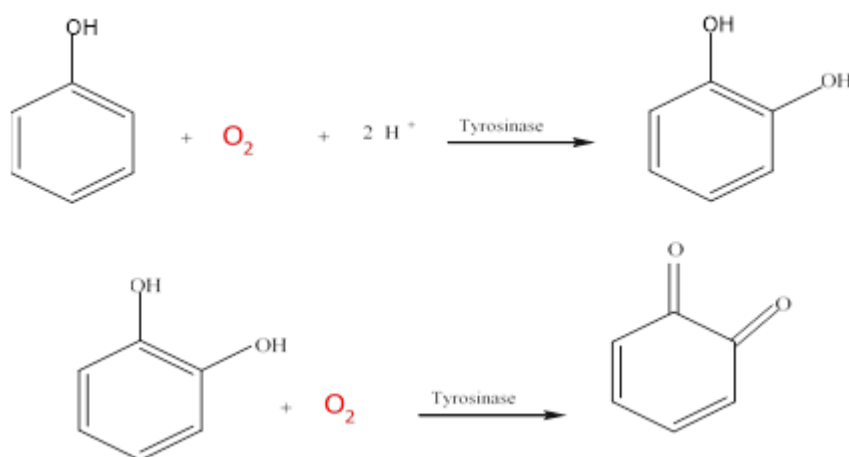

Figure 10. Formation of o-quinone from phenol.

The results shown in **Figure 11(a-f)** and **Table 11** indicate that the 2L/1CuSO₄ complex exhibits the highest reaction rate, with V = 3.31 µmol/K/min. This complex benefits from an optimal 2:1 ratio between the pyrazole ligand and copper, ensuring good stability and accessibility of the catalytic center. Additionally, the presence of a small and weakly coordinating counter-ion (SO₄²⁻) facilitates coordination, further enhancing catalytic performance. In contrast, extreme ratios (3L/1M or 1L/3M) lead to a significant decrease in activity due to steric hindrance or oversaturation of the metal, limiting substrate access to the active site. In conclusion, this study highlights the importance of rationally selecting both the ligand-to-metal ration and the nature of catalysts based on such coordination complexes.
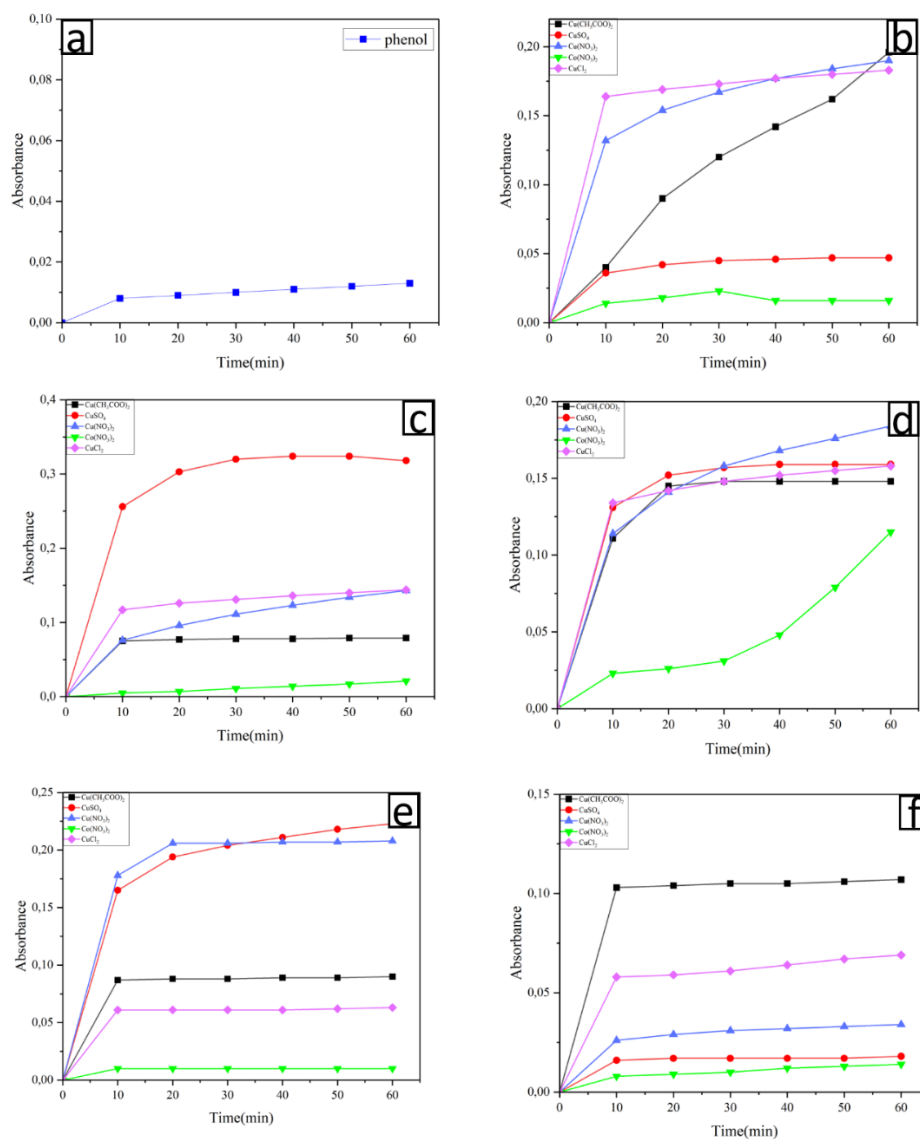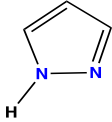
Figure 11. Oxidation of phenol (a) in the presence of complexes formed in situ by 1L/1M (b); 2L/1M (c); 3L/1M (d); 1L/2M (e); 1L/3M (f) in MeOH.

Table 11. Kinetic data for the oxidation of phenol by complexes based on pyrazole and different metal salts in methanol [rate: V (μmol. L^{-1}.min^{-1}), Catalytic activity concentration b (μmol. L^{-1}. min^{-1}), activity: a (μmol mg^{-1}.min^{-1}), and turnover: T (min^{-1})].

Ligands	Sels métalliques	V (μmol/L.min)	b (μmol/mL.min)	b (μmol/mL.min)	T (min^{-1})
	1L/1Cu (CH$_3$COO)$_2$	2.04	15.65	39.19	78.25
	2L/1CuSO$_4$	3.31	25.39	30.83	12695
	3L/1Cu (NO$_3$)$_2$	1.91	14.69	39.15	7345
	1L/2CuSO$_4$	2.32	17.80	35.64	8900
	1L/3Cu (CH$_3$COO)$_2$	1.11	8.54	21.38	4270

The spectrum of the evolution of o-quinone absorbance as a function of time was recorded 10 minutes after the reaction, and the spectrum shown in the figure was obtained in **(Figure 12)**. if we closely examine this spectrum, an increase in absorbance at 390 nm is observed. This increase corresponds to the appearance of o-quinone, which indicates that the copper complex formed by the combination of 2 equivalents of ligand and 1 equivalent of metal (ligand pyrazole and the salt CuSO$_4$) is the best catalyst among our complexes. It exhibits dual activity: catecholase activity (catalysing the oxidation of catechol to o-quinone), and tyrosinase activity (catalysing the oxidation of phenol to catechol).
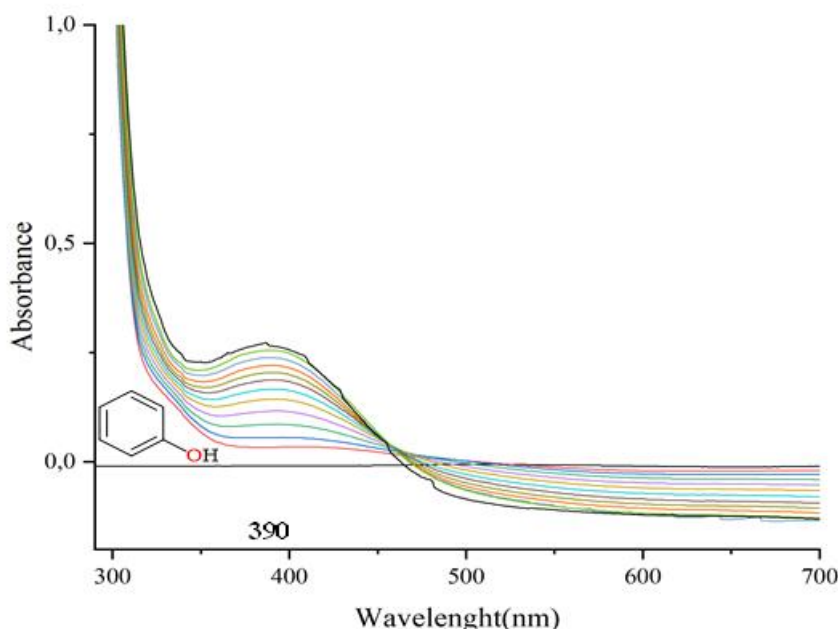

Figure 12. Phenol absorbance recorded at a time interval of 10 min combination 2L/1CuSO$_4$.

3.5. Phenol: Kinetic Study

A kinetic study was performed to determine the Michaelis-Menten constants, Km and Vmax, for the phenol oxidation reaction. This was done by plotting the initial reaction rate (V$_0$) as a function of the catechol substrate concentration. The study was conducted using a solution of the in situ prepared complex, with catechol concentrations ranging from 10^{-2} mol L^{-1} to 6×10^{-1} mol L^{-1} under ambient conditions. To determine Km and Vmax graphically, we used Michaelis-Menten plots, which allow for more accurate extrapolation of these constants. The reaction kinetics followed a typical Michaelis-Menten pattern, as shown in the **Table 12** and **Table 13**. The K$_m$ values range from 0.002 mol·L^{-1} in ACN of the combinations L$_1$/CuCl$_2$, which appears to be the most suitable solvent for the catalytic study of this ligand series with respect to Aminophenol oxidation.

Table 12. Kinetic parameters of the reaction.

ACN	Cu (CH$_3$COO)$_2$	CuSO4	Cu (NO$_3$)$_2$	Co (NO$_3$)$_2$	CuCl$_2$
V$_{max (MeOH)}$	7.92	16.63	17.67	15.69	15.59
K$_{m (MeOH)}$	0.02	0.19	0.17	0.20	0.03
V$_{max (THF)}$	19.25	25.98	15.02	10.43	6.74
K$_{m (THF)}$	0.24	0.25	0.27	0.29	0.009

Table 12 (continue). Kinetic parameters of the reaction.

ACN	Cu (CH₃COO)₂	CuSO4	Cu (NO₃)₂	Co (NO₃)₂	CuCl₂
$V_{max\ (ACN)}$	34.64	2.55	7.68	4.73	13.19
$K_{m\ (ACN)}$	0.08	0.012	0.016	0.27	0.002

Table 13. Dependence of the reaction rates on the phenol (2 ml) concentrations varying 10-1 M to 6 × 10-1 M for the oxidation reaction catalysed by L/M complexes (0.3 ml; 2× 10-3 M) at 290 nm.

Solution	Dependence of the reaction rates
MeOH	
THF	
ACN	
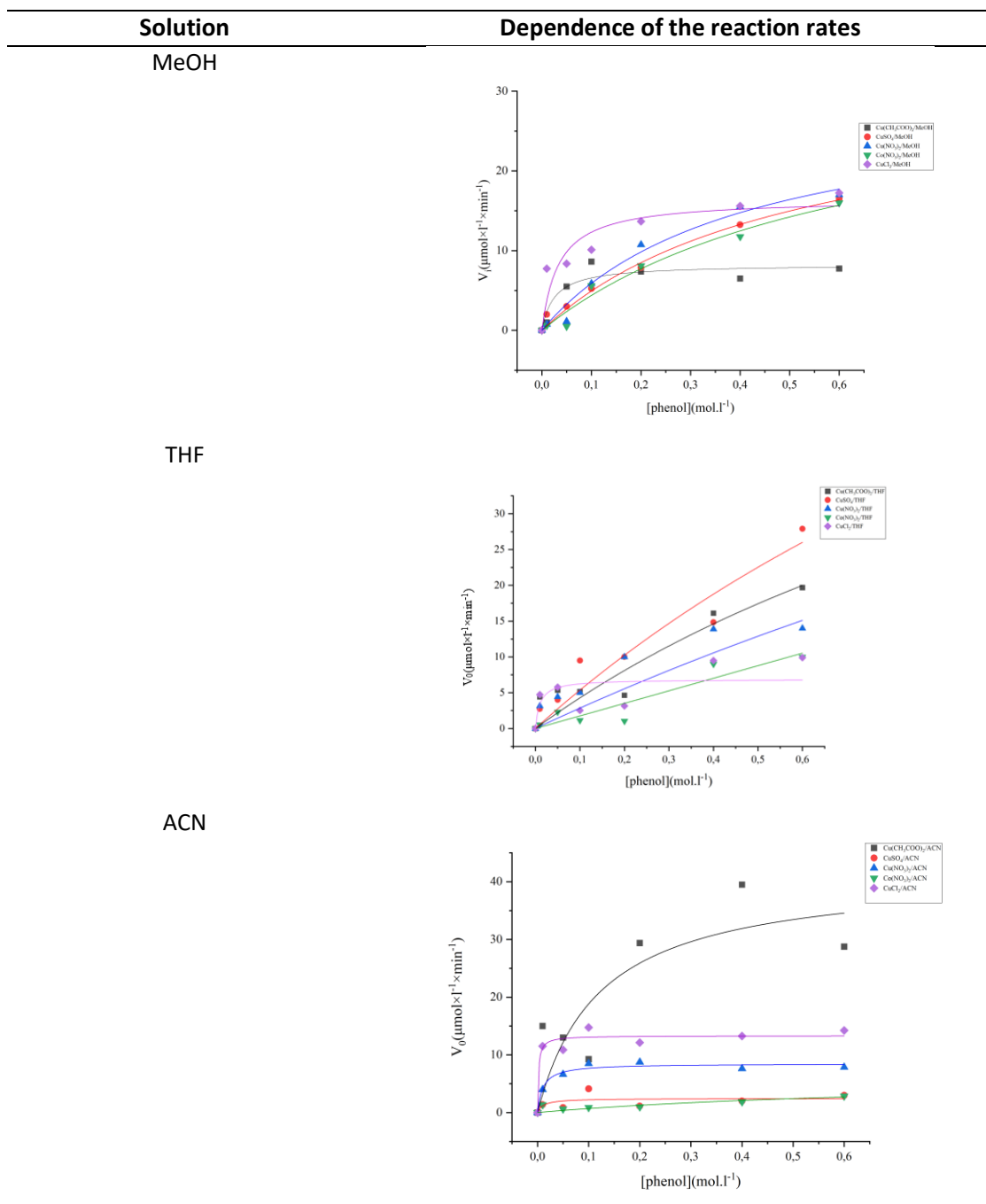
3.6. Phenol: Oxidation of 2,6-Dimethylphenol in the Presence of a Complex in Situ

We aimed to verify that under the experimental conditions used, the 2,6-Dimethylphenol does not oxidize in the absence of the catalyst based on complexes. Scheme 5 thus shows that the absorbances of 3,3',5,5'Tetramethyldiphenoquinone, which should appear at 413 nm in methanol, are almost negligible in the absence of the catalyst (see **Figure 13**).
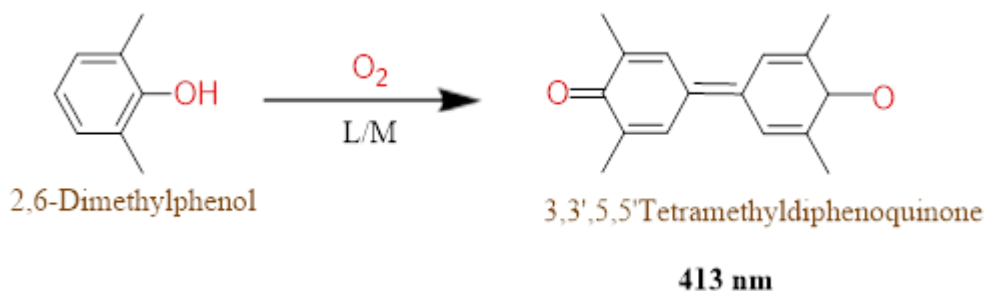

Figure 13. Reaction model.

The kinetic study of 2,6-dimethylphenol oxidation shows that the reaction efficiency strongly depends on the molar ratio between pyrazole (ligand) and the metal salts. The results shown in **Figure 14(a-f)** and **Table 14** indicate that the $2L/1CuSO_4$ complex exhibits the highest reaction rate, with V = 3.31 µmol/L.min. This complex benefits from an optimal 2:1 ratio between the pyrazole ligand and copper, ensuring good stability and accessibility of the catalytic center. Additionally, the presence of a small and weakly coordinating counter-ion (SO_4^{2-}) facilitates coordination, further enhancing catalytic performance. In contrast, ratios with excess pyrazole (2L/1M, 3L/1M) or a moderate excess of metal (1L/1M, 1L/2M) show reduced catalytic activity, likely due to metal site saturation by the ligand or the formation of less reactive complexes. These observations confirm that both the type of metal and the ligand-to-metal ratio have a significant impact on the reactivity and catalytic efficiency of the system. The spectrum showing the evolution of 3,3',5,5'-Tetramethyldiphenoquinone absorbance over time was recorded 10 minutes after the reaction.

Table 14. Kinetic data for the oxidation of 2,6-Dimethylphenol by complexes based on pyrazole and different metal salts in methanol [rate: V (µmol/L.min), Catalytic activity concentration b (µmol/L.min), activity: a (µmol/mg.min), and turnover: T (min⁻¹)].

Ligands	Sels métalliques	V (µmol/L.min)	b (µmol/mL.min)	b (µmol/mL.min)	T (min⁻¹)
	1L/1Cu (CH₃COO)₂	18.75	143.75	360	71875
	2L/1CuSO₄	16.48	126.42	370.75	63210
	3L/1Cu (NO₃)₂	11.52	88.32	221.18	44160
	1L/2CuSO₄	12.90	98.94	247.78	49470
	1L/3Cu (CH₃COO)₂	18.83	144.38	361.58	72190

The resulting spectrum is presented in **Figure 15.** Upon close examination, an increase in absorbance at 413 nm is observed. This increase corresponds to the formation of 3,3',5,5'-Tetramethyldiphenoquinone, indicating that the copper complex formed from the combination of one equivalent of pyrazole ligand and three equivalents of copper (II) acetate [Cu (CH₃COO)₂] is the most efficient catalyst among the studied complexes.
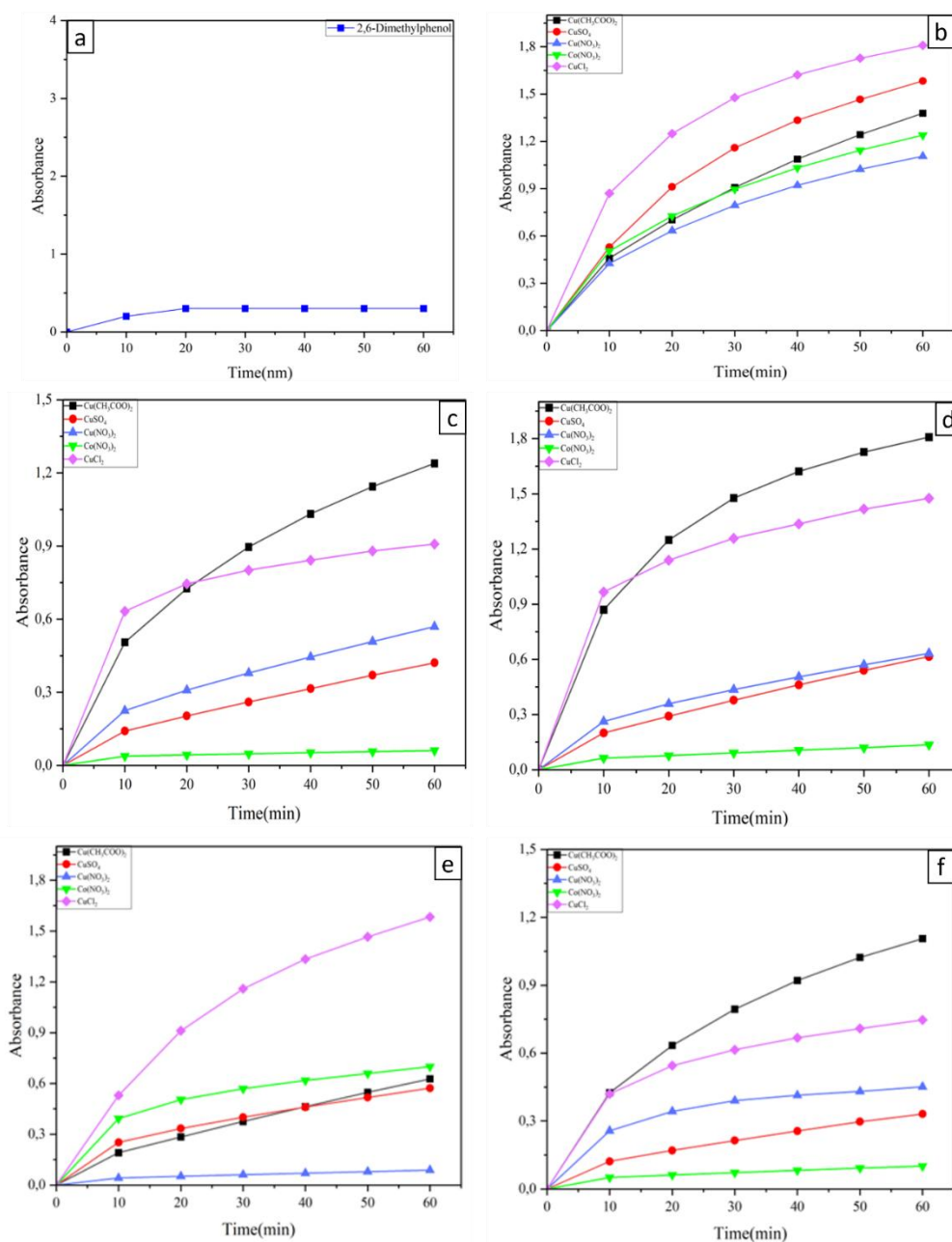
Figure 14. Oxidation of 2,6-Dimethylphenol (a) in the presence of complexes formed in situ by 1L/1M (b); 2L/1M (c); 3L/1M (d); 1L/2M (e); 1L/3M (f) in MeOH.
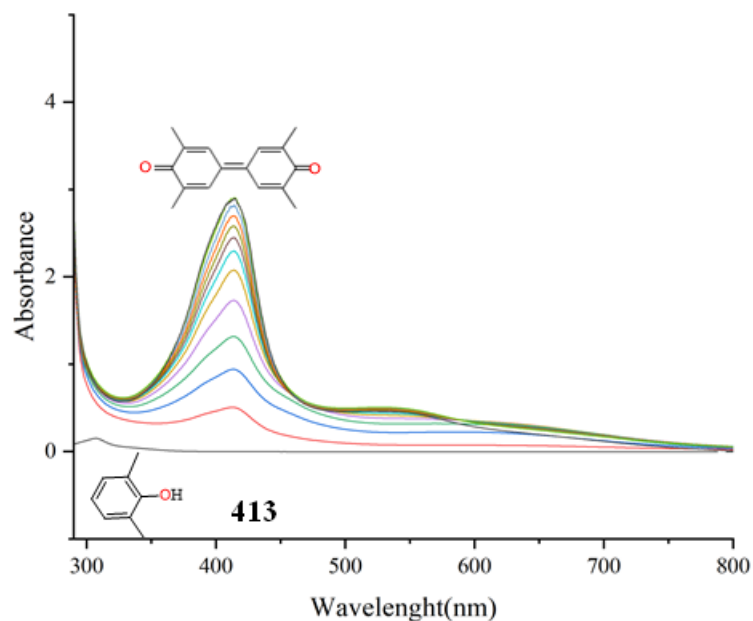
Figure 15. 2,6-Dimethylphenol absorbance recorded at a time interval of 10 min combination 1L/3Cu $(CH_3COO)_2$.

3.7. 2,6-Dimethylphenol: Kinetic Study

Table 15 clearly shows that the values of Km differ with the change of solvent; they range from 0.003 mol/L (L_1/Cu $(NO_3)_2$) for ACN, which represents the best solvent for the catalytic study.

To determine the constants KM and Vmax of the oxidation reaction of 2,6-Dimethylphenol in three different solvents (methanol, THF, acetonitrile), the initial rate method V_0 was used. The first step of this method involves plotting a graph representing the values of V_0 as a function of substrate concentration (**Table 16**). For this combination (1L/1M) were treated with various concentrations of 2,6-Dimethylphenol ranging from 0.01 to 0.6 mol/L, under ambient conditions.

Table 16. Kinetic parameters of the reaction.

ACN	Cu $(CH_3COO)_2$	CuSO4	Cu $(NO_3)_2$	Co $(NO_3)_2$	CuCl₂
$V_{max\,(MeOH)}$	202.91	36.20	40.31	11.37	38.11
$K_{m\,(MeOH)}$	0.20	0.18	0.19	0.191	0.018
$V_{max\,(THF)}$	26.95	81.12	19.99	15.91	23.59
$K_{m\,(THF)}$	0.20	0.08	0.10	0.24	0.13
$V_{max\,(ACN)}$	73.13	11.47	57.33	10.36	138.55
$K_{m\,(ACN)}$	0.007	0.10	0.003	0.20	0.06

Table 16. Dependence of the reaction rates on the 2,6-Dimethylphenol (2 ml) concentrations varying 10-1 M to 6 × 10-1 M for the oxidation reaction catalysed by L/M complexes (0.3 ml; 2× 10-3 M) at 413 nm.

Solution	Dependence of the reaction rates
MeOH	
THF	
ACN	
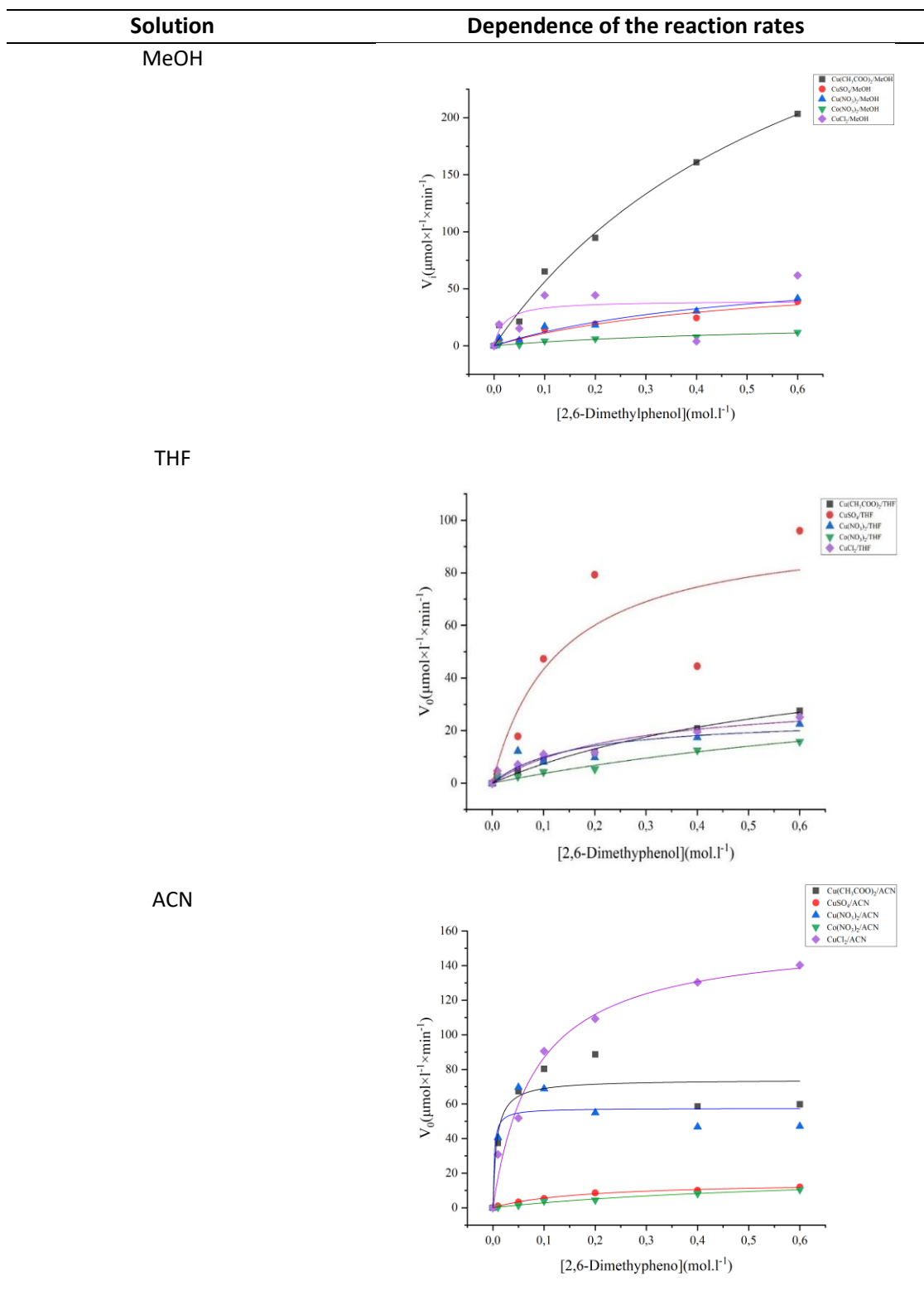
3.8. Proposed Mechanism
3.8.1. Catechol Oxidation Mechanism

The oxidation of catechol to quinone is a key reaction in mimicking catecholase enzyme activity and serves to evaluate the catalytic efficiency of Cu(II)-ligand complexes. This mechanism involves substrate coordination to the metal active site, followed by electron transfer and O_2 activation, leading to quinone and water formation (see **Figure 16**).
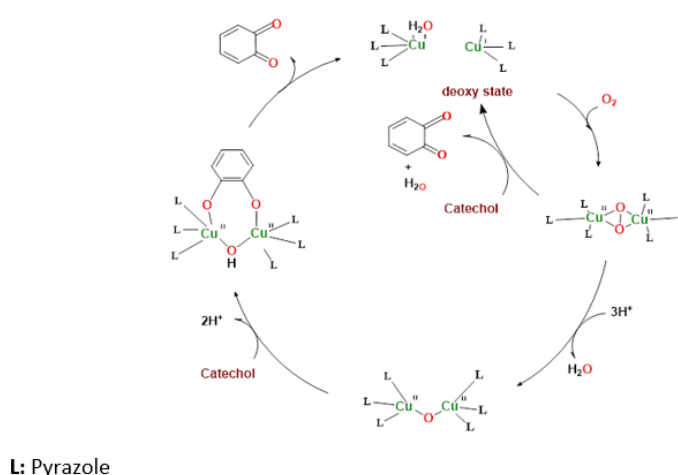

L: Pyrazole

Figure 16. Proposed mechanism for catechol oxidation catalysed by Cu(II)-ligand complexes.

3.8.2. Oxidation Mechanism of 2-aminophenol

The oxidation of 2-aminophenol catalyzed by Cu(II)-ligand complexes is a model reaction simulating tyrosinase activity. This mechanism involves the transformation of 2-aminophenol into 2-aminophenoxazin-3-one through an oxidation and oxidative coupling process, resulting in the appearance of a characteristic absorption band 430 nm, indicative of the tyrosinase-mimetic activity of the studied complex (see **Figure 17**).
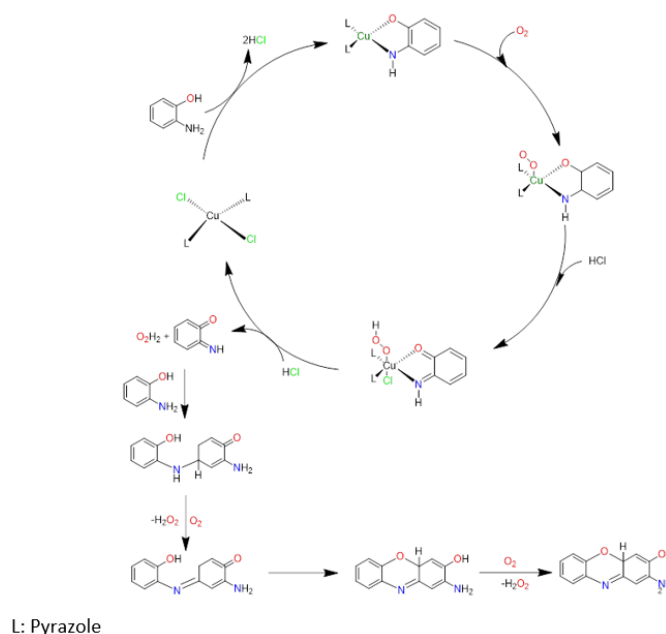

L: Pyrazole

Figure 17. Proposed mechanism for 2-Aminophenol oxidation.

3.8.3. Phenol Oxidation Mechanism

The catalytic oxidation of phenol by Cu(II)-ligand complexes demonstrates their capacity to activate molecular oxygen, leading to catechol formation followed by its conversion to quinone. This reaction is crucial in biomimetic studies, as it evaluates the dual tyrosinase/catecholase activity of synthetic complexes under mild conditions (see **Figure 18**).

3.8.4. 2,6-Dimethylphenol Oxidation Mechanism

2,6-Dimethylphenol is used as a model substrate to evaluate the ability of Cu(II)-ligand complexes to oxidize sterically hindered phenolic compounds. During the reaction, the Cu(II) complex activates molecular oxygen, generating an oxidizing species capable of converting 2,6-dimethylphenol into a phenoxy radical. Due to the methyl groups at positions 2 and 6 causing steric hindrance, radical coupling between two phenoxy radicals preferentially occurs at the 3,3' and 5,5' positions. This coupling leads to the formation of a conjugated dimer, 3,3',5,5'-tetramethyldiphenoquinone, which can be monitored by UV-Vis spectroscopy through a characteristic absorption peak at 413 nm, corresponding to the π-π* transition of the conjugated quinone. This study highlights the steric effects on catalytic activity and the stability of biomimetic complexes during oxygen activation, demonstrating the effectiveness of Cu(II)-ligand complexes for the selective oxidation of hindered phenols (see **Figure 19**).
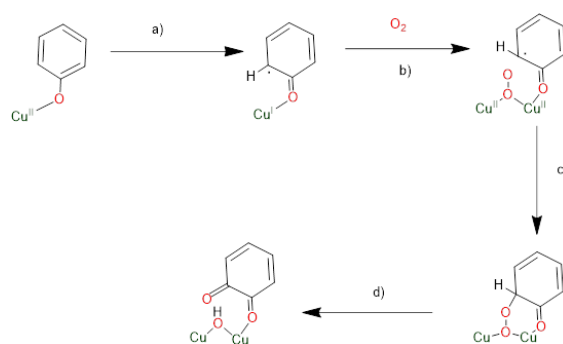

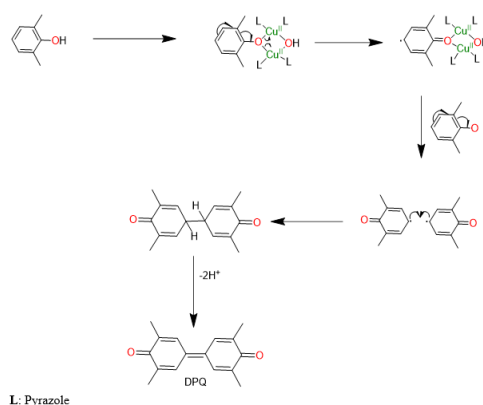
Figure 18. Proposal mechanism for phenol oxidation.

Figure 19. Proposed mechanism for 2,6-Dimethylphenol oxidation.

4. CONCLUSION

This study explores the catalytic potential of copper (II) and cobalt (II) pyrazole-based complexes as biomimetic models for oxidative enzymes such as catecholase, tyrosinase, phenoxazinone synthase, and laccase. The aim was to mimic the natural activation of molecular oxygen to catalyze the oxidation of phenolic substrates including catechol, 2-aminophenol, phenol, and 2,6-dimethylphenol. Complexes were formed in situ using various ligand-to-metal ratios, and their activity was tested under aerobic conditions in different solvents (methanol, THF, and acetonitrile). Characterization using UV-Vis, FTIR, and XRD confirmed the formation and structure of the complexes. The copper-based systems showed significantly higher catalytic efficiency compared to their cobalt counterparts. The best catecholase-like activity was observed with the $1L/3Cu(CH_3COO)_2$ complex in methanol, achieving a rate of 17.156 $\mu mol \cdot L^{-1} \cdot min^{-1}$. For phenoxazinone synthase-like activity, the $1L/2CuSO_4$ complex was the most effective, with a rate of 41.66 $\mu mol \cdot L^{-1} \cdot min^{-1}$. The oxidation of phenol, mimicking tyrosinase activity, was optimal with the $2L/1CuSO_4$ complex. Moreover, the oxidation of 2,6-dimethylphenol was most efficient with the $1L/3CuCl_2$ complex, highlighting the importance of both the metal ion and the ligand-to-metal ratio. Kinetic studies confirmed Michaelis-Menten behavior, with the activity being strongly influenced by the choice of solvent and the coordination environment around the metal. These results demonstrate that pyrazole-metal complexes, especially those with copper (II), are promising candidates for green and selective oxidation catalysis inspired by natural enzymes.

5. ACKNOWLEDGMENT

6. AUTHORS' NOTE

The authors declare that there is no conflict of interest regarding the publication of this article. Authors confirmed that the paper was free of plagiarism.

7. REFERENCES

[1] Alvi, S., Jayant, V., & Ali, R. (2022). Applications of Oxone® in organic synthesis: An emerging green reagent of modern era. *ChemistrySelect*, *7*(23), e202200704.

[2] Arakawa, H., Aresta, M., Armor, J. N., Barteau, M. A., Beckman, E. J., Bell, A. T., and Tumas, W. (2001). Catalysis research of relevance to carbon management: progress, challenges, and opportunities. *Chemical Reviews*, *101*(4), 953-996.

[3] Gligorich, K. M., and Sigman, M. S. (2009). Recent advancements and challenges of palladium II-catalyzed oxidation reactions with molecular oxygen as the sole oxidant. *Chemical communications*, *2009*(26), 3854-3867.

[4] Stahl, S. S. (2004). Palladium oxidase catalysis: selective oxidation of organic chemicals by direct dioxygen-coupled turnover. *Angewandte Chemie International Edition*, *43*(26), 3400-3420.

[5]   Olawade, D. B., Wada, O. Z., Egbewole, B. I., Fapohunda, O., Ige, A. O., Usman, S. O., and Ajisafe, O. (2024). Metal and metal oxide nanomaterials for heavy metal remediation: novel approaches for selective, regenerative, and scalable water treatment. *Frontiers in Nanotechnology*, *6*, 1466721.

[6]   Massey, V. (1994). Activation of molecular oxygen by flavins and flavoproteins. *Journal of Biological Chemistry*, *269*(36), 22459-22462.

[7]   Buglak, A. A., Kapitonova, M. A., Vechtomova, Y. L., and Telegina, T. A. (2022). Insights into molecular structure of pterins suitable for biomedical applications. *International Journal of Molecular Sciences*, *23*(23), 15222.

[8]   Bugg, T. D. (2003). Dioxygenase enzymes: catalytic mechanisms and chemical models. *Tetrahedron*, *59*(36), 7075-7101.

[9]   Thierbach, S., Bui, N., Zapp, J., Chhabra, S. R., Kappl, R., and Fetzner, S. (2014). Substrate-assisted O2 activation in a cofactor-independent dioxygenase. *Chemistry & Biology*, *21*(2), 217-225.

[10] Rolff, M., Schottenheim, J., Decker, H., and Tuczek, F. (2011). Copper–O 2 reactivity of tyrosinase models towards external monophenolic substrates: molecular mechanism and comparison with the enzyme. *Chemical Society Reviews*, *40*(7), 4077-4098.

[11] Itoh, S., and Fukuzumi, S. (2007). Monooxygenase activity of type 3 copper proteins. *Accounts of chemical research*, *40*(7), 592-600.

[12] Parmeggiani, C., and Cardona, F. (2012). Transition metal based catalysts in the aerobic oxidation of alcohols. *Green Chemistry*, *14*(3), 547-564.

[13] Mallat, T., and Baiker, A. (2004). Oxidation of alcohols with molecular oxygen on solid catalysts. *Chemical Reviews*, *104*(6), 3037-3058.

[14] Friedle, S., Reisner, E., AND Lippard, S. J. (2010). Current challenges of modeling diiron enzyme active sites for dioxygen activation by biomimetic synthetic complexes. *Chemical Society Reviews*, *39*(8), 2768-2779.

[15] van den Beuken, E. K., and Feringa, B. L. (1998). Bimetallic catalysis by late transition metal complexes. *Tetrahedron*, *54*(43), 12985-13011.

[16] Titi, A., Dahmani, M., Abbaoui, Z., El Kodadi, M., ET-Touhami, A., Yahyi, A., and Siaj, M. (2024). New catalysts based on carboxylate Sn (IV) complexes used in the oxidation reaction of 3, 5-di-tert-butylcatechol to 3, 5-di-tert-butyl-o-benzoquinone. *Reaction Kinetics, Mechanisms and Catalysis*, *137*(1), 133-148.

[17] Punniyamurthy, T., Velusamy, S., and Iqbal, J. (2005). Recent advances in transition metal catalyzed oxidation of organic substrates with molecular oxygen. *Chemical Reviews*, *105*(6), 2329-2364.

[18] Knorr, L. (1883). Einwirkung von acetessigester auf phenylhydrazin. *Berichte der deutschen chemischen Gesellschaft*, *16*(2), 2597-2599.

[19] v. Pechmann, H. (1898). Pyrazol aus acetylen und diazomethan. *Berichte der deutschen chemischen Gesellschaft*, *31*(3), 2950-2951.

[20] Ojwach, S. O., and Darkwa, J. (2010). Pyrazole and (pyrazol-1-yl) metal complexes as carbon–carbon coupling catalysts. *Inorganica Chimica Acta*, *363*(9), 1947-1964.

[21] Girard, C., Önen, E., Aufort, M., Beauvière, S., Samson, E., amd Herscovici, J. (2006). Reusable polymer-supported catalyst for the [3+ 2] Huisgen cycloaddition in automation protocols. *Organic Letters*, *8*(8), 1689-1692.

[22] Gong, Y. D., and Lee, T. (2010). Combinatorial syntheses of five-membered ring heterocycles using carbon disulfide and a solid support. *Journal of Combinatorial Chemistry*, *12*(4), 393-409.

[23] Nandiyanto, A.B.D., Ragadhita, R., and Fiandini, M. (2023). Interpretation of Fourier Transform Infrared Spectra (FTIR): A practical approach in the polymer/plastic thermal decomposition. *Indonesian Journal of Science and Technology*, *8*(1), 113-126.

[24] Obinna, E.N. (2022). Physicochemical properties of human hair using Fourier Transform Infra-Red (FTIR) and Scanning Electron Microscope (SEM). *ASEAN Journal for Science and Engineering in Materials*, *1*(2), 71-74.

[25] Nandiyanto, A.B.D., Oktiani, R., and Ragadhita, R. (2019). How to read and interpret FTIR spectroscope of organic material. *Indonesian Journal of Science and Technology*, *4*(1), 97-118.